CHAPTER 6

Wave Propagation in Excitable Systems

The problem of current flow in the axon of a nerve is much more complicated than that of flow in dendritic networks (Chapter 4). Recall from Chapter 5 that the voltage dependence of the ionic currents can lead to excitability and action potentials. In this chapter we show that when an excitable membrane is incorporated into a *nonlinear* cable equation, it can give rise to traveling waves of electrical excitation. Indeed, this property is one of the reasons that the Hodgkin–Huxley equations are so important. In addition to producing a realistic description of a space-clamped action potential, Hodgkin and Huxley showed that this action potential propagates along an axon with a fixed speed, which could be calculated.

However, the nerve axon is but one of many examples of a spatially extended excitable system in which there is propagated activity. For example, propagated waves of electrical or chemical activity are known to occur in skeletal and cardiac tissue, in the retina, in the cortex of the brain, and within single cells of a wide variety of types. In this chapter we describe this wave activity, beginning with a discussion of propagated electrical activity along one-dimensional cables, then concluding with a brief discussion of waves in higher-dimensional excitable systems.

6.1 Brief Overview of Wave Propagation

There is a vast literature on wave propagation in biological systems. In addition to the books by Murray (2002), Britton (1986), and Grindrod (1991), there are numerous articles in journals and books, many of which are cited in this chapter.

There are many different kinds of waves in biological systems. For example, there are waves in excitable systems that arise from the underlying excitability of the cell.

An excitable wave acts as a model of, among other things, the propagation of an action potential along the axon of a nerve or the propagation of a grass fire on a prairie. However, if the underlying kinetics are oscillatory but not excitable, and a large number of individual oscillatory units are coupled by diffusion, the resulting behavior is oscillatory waves and periodic wave trains. In this chapter we focus our attention on waves in excitable media, and defer consideration of the theory of coupled oscillators to Chapters 12 and 18.

We emphasize at the outset that by a *traveling wave* we mean a solution of a partial differential equation on an infinite domain (a fictional object, of course) that travels at constant velocity with fixed shape. It is also helpful to make a distinction between the two most important types of traveling waves in excitable systems. First, there is the wave that looks like a moving plateau, or transition between different levels. If v denotes the wave variable, then ahead of the wave, v is steady at some low value, and behind the wave, v is steady at a higher value (Fig. 6.1A). Such waves are called *traveling fronts*. The second type of wave begins and ends at the same value of v (Fig. 6.1B) and resembles a moving bump. This type of wave is called a *traveling pulse*.

These two wave types can be interpreted in the terminology of the Hodgkin–Huxley fast–slow phase plane discussed in Chapter 5. When the recovery variable is fixed at the steady state, the fast–slow phase plane has two stable steady states, $v = v_r$ and $v = v_e$ (i.e., it is bistable). Under appropriate conditions there exists a traveling front with $v = v_r$ ahead of the wave and $v = v_e$ behind the wave. Thus, the traveling front acts like a zipper, switching the domain from the resting to the excited state. However, if the recovery variable n is allowed to vary, the solution is eventually forced to return to the resting state and the traveling solution becomes a traveling pulse. The primary difference between the traveling front and the traveling pulse is that in the former case there is no recovery (or recovery is static), while in the latter case recovery plays an important dynamic role.

One of the simplest models of biological wave propagation is Fisher's equation. Although this equation is used extensively in population biology and ecology, it is much

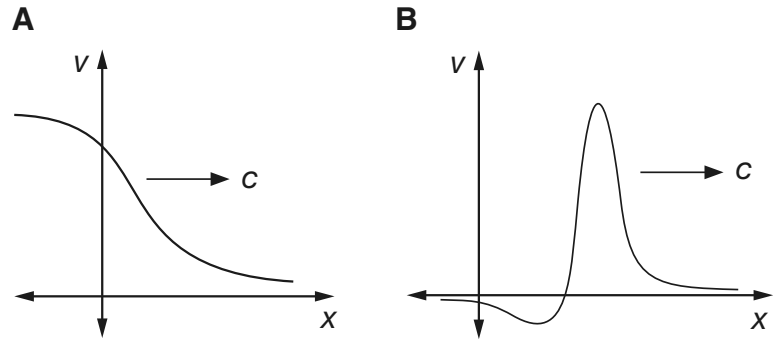

Figure 6.1 Schematic diagram of A: Traveling front, B: Traveling pulse.

less relevant in a physiological context, and so is not discussed here (see Exercise 14 and Fife, 1979).

The next level of complexity is the *bistable equation*. The bistable equation is so named because it has two stable rest points, and it is related to the FitzHugh–Nagumo equations without recovery. For the bistable equation, one expects to find traveling fronts but not traveling pulses. Inclusion of the recovery variable leads to a more complex model, the spatially distributed FitzHugh–Nagumo equations, for which one expects to find traveling pulses (among other types of waves). Wave propagation in the FitzHugh–Nagumo equations is still not completely understood, especially in higher-dimensional domains. At the highest level of complexity are the spatially distributed models of Hodgkin–Huxley type, systems of equations that are resistant to analytical approaches.

6.2 Traveling Fronts

6.2.1 The Bistable Equation

The bistable equation is a specific version of the cable equation (4.18), namely

$$\frac{\partial V}{\partial t} = \frac{\partial^2 V}{\partial x^2} + f(V), \tag{6.1}$$

where $f(V)$ has three zeros at $0, \alpha$, and 1, where $0 < \alpha < 1$. The values $V = 0$ and $V = 1$ are stable steady solutions of the ordinary differential equation $dV/dt = f(V)$. Notice that the variable V has been scaled so that 0 and 1 are zeros of $f(V)$. In the standard nondimensional form, $f'(0) = -1$. (Recall from (4.13) that the passive cable resistance was defined so that the ionic current has slope 1 at rest.) However, this restriction on $f(V)$ is often ignored.

An example of such a function can be found in the Hodgkin–Huxley fast–slow phase plane. When the recovery variable n is held fixed at its steady state, the Hodgkin–Huxley fast–slow model is bistable. Two other examples of functions that are often used in this context are the cubic polynomial

$$f(V) = aV(V-1)(\alpha - V), \qquad 0 < \alpha < 1, \tag{6.2}$$

and the piecewise-linear function

$$f(V) = -V + H(V - \alpha), \qquad 0 < \alpha < 1. \tag{6.3}$$

where $H(V)$ is the Heaviside function (Mckean, 1970). This piecewise-linear function is not continuous, nor does it have three zeros, yet it is useful in the study of traveling wave solutions of the bistable equation because it is an analytically tractable model that retains many important qualitative features.

By a traveling wave solution, we mean a translation-invariant solution of (6.1) that provides a transition between the two stable rest states (zeros of the nonlinear function

$f(V)$) and travels with constant speed. That is, we seek a solution of (6.1) of the form

$$V(x,t) = U(x+ct) = U(\xi) \tag{6.4}$$

for some (yet to be determined) value of c. The new variable ξ, called the traveling wave coordinate, has the property that fixed values move with fixed speed c. When written as a function of ξ, the wave appears stationary. Note that, because we use $\xi = x + ct$ as the traveling wave coordinate, a solution with c positive corresponds to a wave moving from right to left. We could equally well have used $x - ct$ as the traveling wave coordinate, to obtain waves moving from left to right (for positive c).

By substituting (6.4) into (6.1) it can be seen that any traveling wave solution must satisfy

$$U_{\xi\xi} - cU_\xi + f(U) = 0, \tag{6.5}$$

and this, being an ordinary differential equation, should be easier to analyze than the original partial differential equation. For $U(\xi)$ to provide a transition between rest points, it must be that $f(U(\xi)) \to 0$ as $\xi \to \pm\infty$.

It is convenient to write (6.5) as two first-order equations,

$$U_\xi = W, \tag{6.6}$$

$$W_\xi = cW - f(U). \tag{6.7}$$

To find traveling front solutions for the bistable equation, we look for a solution of (6.6) and (6.7) that connects the rest points $(U,W) = (0,0)$ and $(U,W) = (1,0)$ in the (U,W) phase plane. Such a trajectory, connecting two different steady states, is called a heteroclinic trajectory, and in this case is parameterized by ξ; the trajectory approaches $(0,0)$ as $\xi \to -\infty$ and approaches $(1,0)$ as $\xi \to +\infty$ (see the dashed line in Fig. 6.2A). The steady states at $U = 0$ and $U = 1$ are both saddle points, while for the steady state $U = \alpha$, the real part of both eigenvalues have the same sign, negative if c is positive and positive if c is negative, so that this is a node or a spiral point. Since the points at $U = 0$ and $U = 1$ are saddle points, the goal is to determine whether the parameter c can be chosen so that the trajectory that leaves $U = 0$ at $\xi = -\infty$ connects with the saddle point $U = 1$ at $\xi = +\infty$. This mathematical procedure is called *shooting*, and some sample trajectories are shown in Fig. 6.2A.

First, we can determine the sign of c. Supposing a monotone increasing ($U_\xi > 0$) connecting trajectory exists, we multiply (6.5) by U_ξ and integrate from $\xi = -\infty$ to $\xi = \infty$ with the result that

$$c\int_{-\infty}^{\infty} W^2\,d\xi = \int_0^1 f(u)\,du. \tag{6.8}$$

In other words, if a traveling wave solution exists, then the sign of c is the same as the sign of the area under the curve $f(u)$ between $u = 0$ and $u = 1$. If this area is positive, then the traveling solutions move the state variable U from $U = 0$ to $U = 1$, and the state at $U = 1$ is said to be *dominant*. In both of the special cases (6.2) and (6.3), the state $U = 1$ is dominant if $\alpha < 1/2$.

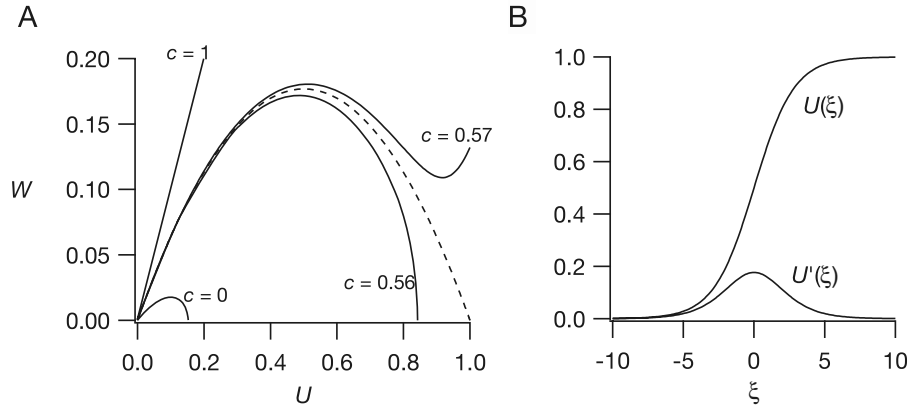

Figure 6.2 A: Trajectories in the (U, W) phase plane leaving the rest point $U = 0$, $W = 0$ for the equation $U_{\xi\xi} - cU_\xi + U(U - 0.1)(1 - U) = 0$, with $c = 0.0$, 0.56, 0.57, and 1.0. Dashed curve shows the connecting heteroclinic trajectory. B: Profile of the traveling wave solution of panel A. In the original coordinates, this front moves to the left with speed c.

Suppose $\int_0^1 f(u)\,du > 0$. We want to determine what happens to the unstable trajectory that leaves the saddle point $U = 0, U_\xi = 0$ for different values of c. With $c = 0$, an explicit expression for this trajectory is found by multiplying (6.5) by U_ξ and integrating to get

$$\frac{W^2}{2} + \int_0^U f(u)\,du = 0. \tag{6.9}$$

If this trajectory were to reach $U = 1$ for some value of W, then

$$\frac{W^2}{2} + \int_0^1 f(u)\,du = 0, \tag{6.10}$$

which can occur only if $\int_0^1 f(u)\,du \le 0$. Since this contradicts our assumption that $\int_0^1 f(u)\,du \ge 0$, we conclude that this trajectory cannot reach $U = 1$. Neither can this trajectory remain in the first quadrant, as $W > 0$ implies that U is increasing. Thus, this trajectory must intersect the $W = 0$ axis at some value of $U < 1$ (Fig. 6.2A). It cannot be the connecting trajectory.

Next, suppose c is large. In the (U, W) phase plane, the slope of the unstable trajectory leaving the rest point at $U = 0$ is the positive root of $\lambda^2 - c\lambda + f'(0) = 0$, which is always larger than c (Exercise 1). Let K be the smallest positive number for which $f(u)/u \le K$ for all u on the interval $0 < u \le 1$ (Exercise: How do we know K exists?), and let σ be any fixed positive number. On the line $W = \sigma U$ the slope of trajectories satisfies

$$\frac{dW}{dU} = c - \frac{f(U)}{W} = c - \frac{f(U)}{\sigma U} \ge c - \frac{K}{\sigma}. \tag{6.11}$$

By picking c large enough, we are assured that $c - K/\sigma > \sigma$, so that once trajectories are above the line $W = \sigma U$, they stay above it. We know that for large enough c, the trajectory leaving the saddle point $U = 0$ starts out above this curve. Thus, this trajectory always stays above the line $W = \sigma U$, and therefore passes above the rest point at $(U, W) = (1, 0)$.

Now we have two trajectories, one with $c = 0$, which misses the rest point at $U = 1$ by crossing the $W = 0$ axis at some point $U < 1$, and one with c large, which misses this rest point by staying above it at $U = 1$. Since trajectories depend continuously on the parameters of the problem, there is a continuous family of trajectories depending on the parameter c between these two special trajectories, and therefore there is at least one trajectory that hits the point $U = 1, W = 0$ exactly.

The value of c for which this heteroclinic connection occurs is unique. To verify this, notice from (6.11) that the slope dW/dU of trajectories in the (U, W) plane is a monotone increasing function of the parameter c. Suppose at some value of $c = c_0$ there is known to be a connecting trajectory. For any value of c that is larger than c_0, the trajectory leaving the saddle point at $U = 0$ must lie above the connecting curve for c_0. For the same reason, with $c > c_0$, the trajectory approaching the saddle point at $U = 1$ as $\xi \to \infty$ must lie below the connecting curve with $c = c_0$. A single curve cannot simultaneously lie above and below another curve, so there cannot be a connecting trajectory for $c > c_0$. By a similar argument, there cannot be a connecting trajectory for a smaller value of c, so the value c_0, and hence the connecting trajectory, is unique.

For most functions $f(V)$, it is necessary to calculate the speed of propagation of the traveling front solution numerically. However, in the two special cases (6.2) and (6.3) the speed of propagation can be calculated explicitly. In the piecewise linear case (6.3) one calculates directly that

$$c = \frac{1 - 2\alpha}{\sqrt{\alpha - \alpha^2}} \tag{6.12}$$

(see Exercise 4).

Suppose $f(u)$ is the cubic polynomial

$$f(u) = -A^2(u - u_0)(u - u_1)(u - u_2), \tag{6.13}$$

where the zeros of the cubic are ordered $u_0 < u_1 < u_2$. We want to find a heteroclinic connection between the smallest zero, u_0, and the largest zero, u_2, so we guess that

$$W = -B(U - u_0)(U - u_2). \tag{6.14}$$

We substitute this guess into the governing equation (6.5), and find that we must have

$$B^2(2U - u_0 - u_2) - cB - A^2(U - u_1) = 0. \tag{6.15}$$

This is a linear function of U that can be made identically zero only if we choose $B = A/\sqrt{2}$ and

$$c = \frac{A}{\sqrt{2}}(u_2 - 2u_1 + u_0). \tag{6.16}$$

It follows from (6.14) that

$$U(\xi) = \frac{u_0 + u_2}{2} + \frac{u_2 - u_0}{2} \tanh\left(\frac{A}{\sqrt{2}} \frac{u_2 - u_0}{2} \xi\right), \tag{6.17}$$

which is independent of u_1. In the case that $u_0 = 0, u_1 = \alpha$, and $u_2 = 1$, the speed reduces to

$$c = \frac{A}{\sqrt{2}}(1 - 2\alpha), \tag{6.18}$$

showing that the speed is a decreasing function of α and the direction of propagation changes at $\alpha = 1/2$. The profile of the traveling wave in this case is

$$U(\xi) = \frac{1}{2}\left[1 + \tanh\left(\frac{A}{2\sqrt{2}}\xi\right)\right]. \tag{6.19}$$

A plot of this traveling wave profile is shown in Fig. 6.2B.

Once the solution of the nondimensional cable equation (6.1) is known, it is a simple matter to express the solution in terms of physical parameters as

$$V(x,t) = U\left(\frac{x}{\lambda_m} + c\frac{t}{\tau_m}\right), \tag{6.20}$$

where λ_m and τ_m are, respectively, the space and time constants of the cable, as described in Chapter 4. The speed of the traveling wave is

$$s = \frac{c\lambda_m}{\tau_m} = \frac{c}{2C_m}\sqrt{\frac{d}{R_m R_c}}, \tag{6.21}$$

which shows how the wave speed depends on capacitance, membrane resistance, cytoplasmic resistance, and axonal diameter. The dependence of the speed on ionic channel conductances is contained (but hidden) in c. According to empirical measurements, a good estimate of the speed of an action potential in an axon is

$$s = \sqrt{\frac{d}{10^{-6}\text{m}}}\ \text{m/sec}. \tag{6.22}$$

Using $d = 500\ \mu$m for squid axon, this estimate gives $s = 22.4$ mm/ms, which compares favorably to the measured value of $s = 21.2$ mm/ms.

Scaling arguments can also be used to find the dependence of speed on certain other parameters. Suppose, for example, that a drug is applied to the membrane that blocks a percentage of all ion channels, irrespective of type. If ρ is the fraction of remaining operational channels, then the speed of propagation is reduced by the factor $\sqrt{\rho}$. This follows directly by noting that the bistable equation with a reduced number of ion channels,

$$V'' - sV' + \rho f(V) = 0, \tag{6.23}$$

can be related to the original bistable equation (6.5) by taking $V(\xi) = U(\sqrt{\rho}\xi), s = c\sqrt{\rho}$.

Table 6.1 Sodium channel densities in selected excitable tissues.

Tissue	Channel density (channels/μm^2)
Mammalian	
Vagus nerve (nonmyelinated)	110
Node of Ranvier	2100
Skeletal muscle	205–560
Other animals	
Squid giant axon	166–533
Frog sartorius muscle	280
Electriceel electroplax	550
Garfish olfactory nerve	35
Lobster walking leg nerve	90

Thresholds and Stability

There are many other features of the bistable equation, the details of which are beyond the scope of this book. Perhaps the most important of these features is that solutions of the bistable equation satisfy a comparison property: any two solutions of the bistable equation, say $u_1(x,t)$ and $u_2(x,t)$, that are ordered with $u_1(x,t_0) \leq u_2(x,t_0)$ at some time $t = t_0$, remain ordered for all subsequent times, i.e., $u_1(x,t) \leq u_2(x,t)$ for $t \geq t_0$.

With comparison arguments it is possible to prove a number of additional facts (Aronson and Weinberger, 1975). For example, the bistable equation exhibits threshold behavior. Specifically, if initial data are sufficiently small, then the solution of the bistable equation approaches zero in the limit $t \to \infty$. However, there are initial functions with compact support lying between 0 and 1 for which the solution approaches 1 in the limit $t \to \infty$. Because of the comparison theorem any larger initial function also initiates a solution that approaches 1 in the limit $t \to \infty$. Such initial data are said to be *superthreshold*.

Furthermore, the traveling wave solution of the bistable equation is stable in a very strong way (Fife, 1979; Fife and McLeod, 1977), as follows. Starting from any initial data that lie between 0 and α in the limit $x \to -\infty$ and between α and 1 in the limit $x \to \infty$, the solution approaches some phase shift of the traveling wave solution in the limit of large time.

6.2.2 Myelination

Most nerve fibers are coated with a lipid material called *myelin* with periodic gaps of exposure called *nodes of Ranvier* (Fig. 6.3). The myelin sheath consists of a single cell, called a *Schwann cell*, which is wrapped many times (roughly 100 times) around the axonal membrane. This wrapping of the axon increases the effective membrane resistance by a factor of about 100 and decreases the membrane capacitance by a factor of about 100. Indeed, rough data are that R_m is 10^3 Ω cm^2 for cell membrane

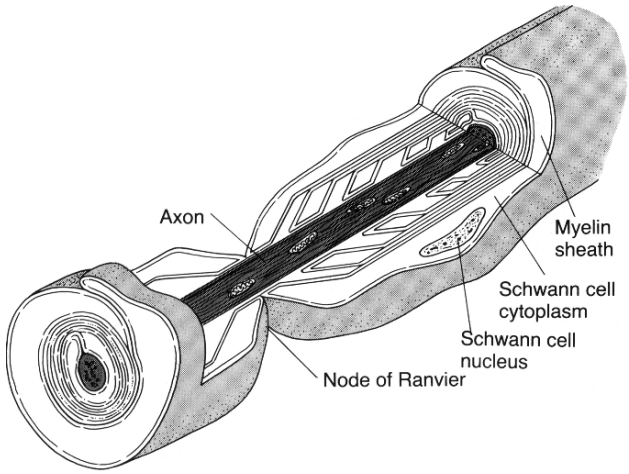

Figure 6.3 Schematic diagram of the myelin sheath. (Guyton and Hall, 1996, Fig. 5–16, p. 69.)

and $10^5\ \Omega\,\mathrm{cm}^2$ for myelin sheath, and that C_m is $10^{-6}\ \mu\mathrm{F/cm}^2$ for cell membrane and $10^{-8}\ \mu\mathrm{F/cm}^2$ for a myelinated fiber. The length of myelin sheath is typically 1 to 2 mm (close to 100 d, where d is the fiber diameter), and the width of the node of Ranvier is about 1 μm.

Propagation along myelinated fiber is faster than along nonmyelinated fiber. This is presumably caused by the fact that there is little transmembrane ionic current and little capacitive current in the myelinated section, allowing the axon to act as a simple resistor. An action potential does not propagate along the myelinated fiber but rather jumps from node-to-node. This node-to-node propagation is said to be *saltatory* (from the Latin word *saltare*, to leap or dance).

The pathophysiological condition of nerve cells in which damage of the myelin sheath impairs nerve impulse transmission in the central nervous system is called *multiple sclerosis*. Multiple sclerosis is an autoimmune disease that usually affects young adults between the ages of 18 and 40, occurring slightly more often in females than males. With multiple sclerosis, there is an immune response to the white matter of the brain and spinal cord, causing demyelination of nerve fibers at various locations throughout the central nervous system, although the underlying nerve axons and cell bodies are not usually damaged. The loss of myelin slows or stops the transmission of action potentials, with the resultant symptoms of muscle fatigue and weakness or extreme "heaviness."

To model the electrical activity in a myelinated fiber we assume that the capacitive and transmembrane ionic currents are negligible, so that, along the myelin sheath, the axial currents

$$I_e = -\frac{1}{r_e}\frac{\partial V_e}{\partial x}, \qquad I_i = -\frac{1}{r_i}\frac{\partial V_i}{\partial x} \tag{6.24}$$

are constant (using the same notation as in Chapter 4). We also assume that V does not vary within each node of Ranvier (i.e., that the nodes are isopotential), and that

V_n is the voltage at the nth node. Then the axial currents between node n and node $n+1$ are

$$I_e = -\frac{1}{Lr_e}(V_{e,n+1} - V_{e,n}), \qquad I_i = -\frac{1}{Lr_i}(V_{i,n+1} - V_{i,n}), \tag{6.25}$$

where L is the length of the myelin sheath between nodes. The total transmembrane current at a node is given by

$$\begin{aligned} \mu p\left(C_m \frac{\partial V_n}{\partial t} + I_{\text{ion}}\right) &= I_{i,n} - I_{i,n+1} \\ &= \frac{1}{L(r_i + r_e)}(V_{n+1} - 2V_n + V_{n-1}), \end{aligned} \tag{6.26}$$

where μ is the length of the node.

We can introduce dimensionless time $\tau = \frac{t}{C_m R_m} = t/\tau_m$ (but not dimensionless space), to rewrite (6.26) as

$$\frac{dV_n}{d\tau} = f(V_n) + D(V_{n+1} - 2V_n + V_{n-1}), \tag{6.27}$$

where $D = \frac{R_m}{\mu L p(r_i + r_e)}$ is the coupling coefficient. We call this equation the *discrete cable equation*.

6.2.3 The Discrete Bistable Equation

The discrete bistable equation is the system of equations (6.27) where $f(V)$ has typical bistable form, as, for example, (6.2) or (6.3). The study of the discrete bistable equation is substantially more difficult than that of the continuous version (6.1). While the discrete bistable equation looks like a finite difference approximation of the continuous bistable equation, solutions of the two have significantly different behavior.

It is a highly nontrivial matter to prove that traveling wave solutions of the discrete system exist (Zinner, 1992). However, a traveling wave solution, if it exists, satisfies the special relationship $V_{n+1}(\tau) = V_n(\tau - \tau_d)$. In other words, the $(n+1)$st node experiences exactly the same time course as the nth node, with time delay τ_d. Furthermore, if $V_n(\tau) = V(\tau)$, it follows from (6.27) that $V(\tau)$ must satisfy the delay differential equation

$$\frac{dV}{d\tau} = D(V(\tau + \tau_d) - 2V(\tau) + V(\tau - \tau_d)) + f(V(\tau)). \tag{6.28}$$

If the function $V(\tau)$ is sufficiently smooth and if τ_d is sufficiently small, then we can approximate $V(\tau + \tau_d)$ with its Taylor series $V(\tau + \tau_d) = \sum_{n=0} \frac{1}{n!} V^{(n)}(\tau)\tau_d^n$, so that (6.28) is approximated by the differential equation

$$D\left(\tau_d^2 V_{\tau\tau} + \frac{\tau_d^4}{12} V_{\tau\tau\tau\tau}\right) - V_\tau + f(V) = 0, \tag{6.29}$$

ignoring terms of order τ_d^6 and higher.

Now we suppose that τ_d is small. The leading-order equation is

$$D\tau_d^2 V_{\tau\tau} - V_\tau + f(V) = 0, \tag{6.30}$$

which has solution $V_0(\tau) = U(c\tau)$, provided that $D\tau_d^2 = 1/c^2$, where U is the traveling front solution of the bistable equation (6.5) and c is the dimensionless wave speed for the continuous equation. The wave speed s is the internodal distance $L + \mu$ divided by the time delay $\tau_m \tau_d$, so that

$$s = \frac{L+\mu}{\tau_m \tau_d} = (L+\mu)c\frac{\sqrt{D}}{\tau_m}. \tag{6.31}$$

For myelinated nerve fiber we know that $D = \frac{R_m}{\mu L p(r_i + r_e)}$. If we ignore extracellular resistance, we find a leading-order approximation for the velocity of

$$s = \frac{L+\mu}{\sqrt{\mu L}} \frac{c}{2C_m}\sqrt{\frac{d}{R_m R_c}}, \tag{6.32}$$

giving a change in velocity compared to nonmyelinated fiber by the factor $\frac{L+\mu}{\sqrt{\mu L}}$. With the estimates $L = 100\,d$ and $\mu = 1\ \mu$m, this increase in velocity is by a factor of $10\sqrt{\frac{d}{10^{-6}\text{m}}}$, which is substantial. Empirically it is known that the improvement of velocity for myelinated fiber compared to nonmyelinated fiber is by a factor of about $6\sqrt{\frac{d}{10^{-6}\text{m}}}$.

Higher-Order Approximation

We can find a higher-order approximation to the speed of propagation by using a standard regular perturbation argument. We set $\epsilon = 1/D$ and seek a solution of (6.29) of the form

$$V(\tau) = V_0(\tau) + \epsilon V_1(\tau) + \cdots, \tag{6.33}$$

$$\tau_d^2 = \frac{\epsilon}{c^2} + \epsilon^2 \tau_1 + \cdots. \tag{6.34}$$

We expand (6.29) into its powers of ϵ and set the coefficients of ϵ to zero. The first equation we obtain from this procedure is (6.30), and the second equation is

$$L[V_1] = \frac{1}{c^2}V_1'' - V_1' + f'(V_0)V_1 = -\frac{V_0''''}{12c^4} - \tau_1 V_0''. \tag{6.35}$$

Note that here we are using $L[\cdot]$ to denote a linear differential operator. The goal is to find solutions of (6.35) that are square integrable on the infinite domain, so that the solution is "close" to V_0. The linear operator $L[\cdot]$ is not an invertible operator in this space by virtue of the fact that $L[V_0'(\tau)] = 0$. (This follows by differentiating (6.30) once with respect to τ.) Thus, it follows from the Fredholm alternative theorem (Keener, 1998) that a solution of (6.35) exists if and only if the right-hand side of the equation is orthogonal to the null space of the adjoint operator L^*. Here the adjoint differential operator is

$$L^*[V] = \frac{1}{c^2}V'' + V' + f'(V_0)V, \tag{6.36}$$

and the one element of the null space (a solution of $L^*[V] = 0$) is

$$V^*(\tau) = \exp\left(-c^2\tau\right) V_0'(\tau). \tag{6.37}$$

This leads to the solvability condition

$$\tau_1 \int_{-\infty}^{\infty} \exp\left(-c^2\tau\right) V_0'(\tau) V_0''(\tau)\, d\tau = -\frac{1}{12c^4} \int_{-\infty}^{\infty} \exp\left(-c^2\tau\right) V_0'(\tau) V_0''''(\tau)\, d\tau. \tag{6.38}$$

As a result, τ_1 can be calculated (either analytically or numerically) by evaluating two integrals, and the speed of propagation is determined as

$$s = (L+\mu)\frac{c}{\tau_m}\sqrt{D}\left(1 - \frac{\tau_1 c^2}{2D} + O\left(\frac{c^2}{D}\right)^2\right). \tag{6.39}$$

This exercise is interesting from the point of view of numerical analysis, as it shows the effect of numerical discretization on the speed of propagation. This method can be applied to other numerical schemes for an equation with traveling wave solutions (Exercise 20).

Propagation Failure

The most significant difference between the discrete and continuous equations is that the discrete system has a coupling threshold for propagation, while the continuous model allows for propagation at all coupling strengths. It is readily seen from (6.21) that for the continuous cable equation, continuous changes in the physical parameters lead to continuous changes in the speed of propagation, and the speed cannot be driven to zero unless the diameter is zero or the resistances or capacitance are infinite. Such is not the case for the discrete system, and propagation may fail if the coupling coefficient is too small. This is easy to understand when we realize that if the coupling strength is very weak, so that the effective internodal resistance is large, the current flow from an excited node to an unexcited node may be so small that the threshold of the unexcited node is not exceeded, and propagation cannot continue.

To study propagation failure, we seek standing (time-independent, i.e., $dV_n/d\tau = 0$) solutions of the discrete equation (6.27). The motivation for this comes from the maximum principle and comparison arguments. One can show that if two sets of initial data for the discrete bistable equation are initially ordered, the corresponding solutions remain ordered for all time. It follows that if the discrete bistable equation has a monotone increasing stationary front solution, then there cannot be a traveling wave front solution.

A standing front solution of the discrete bistable equation is a sequence $\{V_n\}$ satisfying the finite difference equation

$$0 = D(V_{n+1} - 2V_n + V_{n-1}) + f(V_n) \tag{6.40}$$

for all integers n, for which $V_n \to 1$ as $n \to \infty$ and $V_n \to 0$ as $n \to -\infty$.

One can show (Keener, 1987) that for any bistable function f, there is a number $D^* > 0$ such that for $D \leq D^*$, the discrete bistable equation has a standing solution, that is, propagation fails. To get a simple understanding of the behavior of this coupling threshold, we solve (6.40) in the special case of piecewise-linear dynamics (6.3). Since the discrete equation with dynamics (6.3) is linear, the homogeneous solution can be expressed as a linear combination of powers of some number λ as

$$V_n = A\lambda^n + B\lambda^{-n}, \tag{6.41}$$

where λ is a solution of the characteristic polynomial equation

$$\lambda^2 - \left(2 + \frac{1}{D}\right)\lambda + 1 = 0. \tag{6.42}$$

Note that this implies that

$$D = \frac{\lambda}{(\lambda - 1)^2}. \tag{6.43}$$

The characteristic equation has two positive roots, one larger and one smaller than 1. Let λ be the root that is smaller than one. Then, taking the conditions at $\pm\infty$ into account, we write the solution as

$$V_n = \begin{cases} 1 + A\lambda^n, & \text{for } n \geq 0, \\ B\lambda^{-n}, & \text{for } n < 0. \end{cases} \tag{6.44}$$

This expression for V_n must also satisfy the piecewise-linear discrete bistable equation for $n = -1, 0$. Thus,

$$D(V_1 - 2V_0 + V_{-1}) = V_0 - 1, \tag{6.45}$$

$$D(V_0 - 2V_{-1} + V_{-2}) = V_{-1}, \tag{6.46}$$

where we have assumed that $V_n \geq \alpha$ for all $n \geq 0$, and $V_n < \alpha$ for all $n < 0$. Substituting in (6.43) for D, and solving for A and B, then gives $B = A + 1 = \frac{1}{1+\lambda}$.

Finally, this is a solution for all n, provided that $V_0 \geq \alpha$. Since $V_0 = B = \frac{1}{1+\lambda}$, we need $\frac{1}{1+\lambda} \geq \alpha$, or $\lambda \leq \frac{1-\alpha}{\alpha}$. However, when $\lambda < 1$, D is an increasing function of λ, and thus $\lambda \leq \frac{1-\alpha}{\alpha}$ whenever

$$D \leq D\left(\frac{1-\alpha}{\alpha}\right) = \frac{\alpha(1-\alpha)}{(2\alpha - 1)^2} = D^*. \tag{6.47}$$

In other words, there is a standing wave, precluding propagation, whenever the coupling is small, with $D \leq D^*$. Since α is a measure of the excitability of this medium, we see that when the medium is weakly excitable (α is near 1/2), then D^* is large and very little resistance is needed to halt propagation. On the other hand, when α is small, so that the medium is highly excitable, the resistance threshold is large, and propagation is relatively difficult to stop.

6.3 Traveling Pulses

A traveling pulse (often called a *solitary pulse*) is a traveling wave solution that starts and ends at the same steady state of the governing equations. Recall that a traveling front solution corresponds to a heteroclinic trajectory in the (U, W) phase plane, i.e., a trajectory, parameterized by ξ, that connects two different steady states of the system. A traveling pulse solution is similar, corresponding to a trajectory that begins and ends at the *same* steady state in the traveling wave coordinate system. Such trajectories are called *homoclinic orbits*.

There are three main approaches to finding traveling pulses for excitable systems. First, one can approximate the nonlinear functions with piecewise-linear functions, and then find traveling pulse solutions as exact solutions of transcendental equations. Second, one can use perturbation methods exploiting the different time scales to find approximate analytical expressions. Finally, one can use numerical simulations to solve the governing differential equations. We illustrate each of these techniques in turn.

6.3.1 The FitzHugh–Nagumo Equations

To understand the structure of a traveling pulse it is helpful first to study traveling pulse solutions in the FitzHugh–Nagumo equations

$$\epsilon \frac{\partial v}{\partial t} = \epsilon^2 \frac{\partial^2 v}{\partial x^2} + f(v, w), \tag{6.48}$$

$$\frac{\partial w}{\partial t} = g(v, w), \tag{6.49}$$

where ϵ is assumed to be a small positive number. Without any loss of generality, space has been scaled so that the diffusion coefficient is ϵ^2. It is important to realize that this does not imply anything about the magnitude of the physical diffusion coefficient. This is simply a scaling of the space variable so that in the new coordinate system, the wave front appears steep, a procedure that facilitates the study of the wave as a whole. The variable v is spatially coupled with diffusion, but the variable w is not, owing to the fact that v represents the membrane potential, while w represents a slow ionic current or gating variable.

To study traveling waves, we place the system of equations (6.48)–(6.49) in a traveling coordinate frame of reference. We define the traveling wave coordinate $\xi = x - ct$, where $c > 0$ is the wave speed, yet to be determined. Note that the traveling wave variable, $\xi = x - ct$, is different from the one previously used in this chapter, $x + ct$. Hence, $c > 0$ here corresponds to a wave moving from left to right.

The partial differential equations (6.48)–(6.49) become the ordinary differential equations

$$\epsilon^2 v_{\xi\xi} + c\epsilon v_\xi + f(v, w) = 0, \tag{6.50}$$

$$c w_\xi + g(v, w) = 0. \tag{6.51}$$

A Piecewise-Linear Model

We begin by examining the simplest case, the piecewise-linear dynamics (Rinzel and Keller, 1973)

$$f(v,w) = H(v-\alpha) - v - w, \tag{6.52}$$

$$g(v,w) = v. \tag{6.53}$$

Because the dynamics are piecewise linear, the exact solution can be constructed in a piecewise manner. We look for solutions of the form sketched in Fig. 6.4. The position of the wave along the ξ axis is specified by fixing $v(0) = v(\xi_1) = \alpha$. As yet, ξ_1 is unknown, and is to be determined as part of the solution process. Note that the places where $v = \alpha$ are those where the dynamics change (since α is the point of discontinuity of f). Let I, II, and III denote, respectively, the regions $\xi < 0$, $0 < \xi < \xi_1$, and $\xi_1 < \xi$. In each region, the differential equation is linear and so can be solved exactly. The three regional solutions are then joined at $\xi = 0$ and $\xi = \xi_1$ by stipulating that v and w be continuous at the boundaries and that v have a continuous derivative there. These constraints are sufficient to determine the solution unambiguously.

In regions I and III, $v < \alpha$, and so the differential equation is

$$\epsilon^2 v_{\xi\xi} + c\epsilon v_\xi - v - w = 0, \tag{6.54}$$

$$cw_\xi + v = 0. \tag{6.55}$$

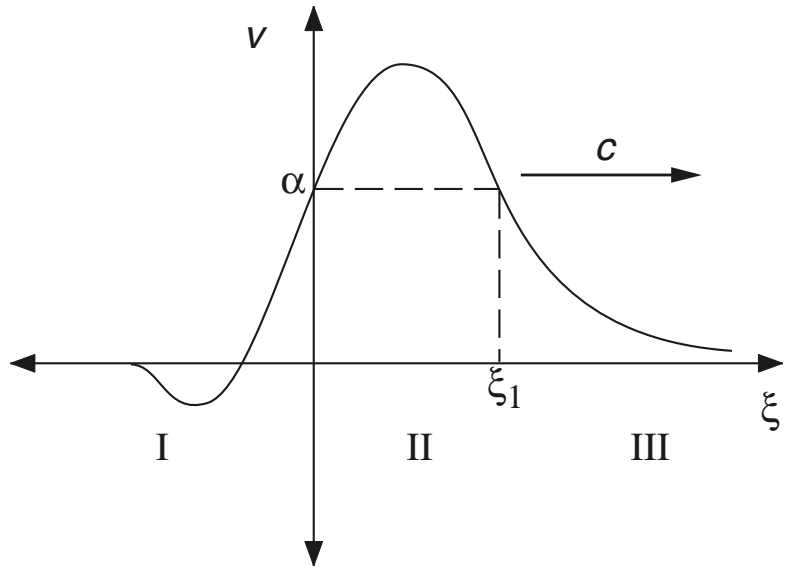

Figure 6.4 Schematic diagram of the traveling pulse of the piecewise-linear FitzHugh–Nagumo equations.

Looking for solutions of the form $v = A\exp(\lambda\xi)$, $w = B\exp(\lambda\xi)$, we find that A and B must satisfy

$$\begin{pmatrix} \lambda^2\epsilon^2 + c\epsilon\lambda - 1 & -1 \\ 1 & c\lambda \end{pmatrix}\begin{pmatrix} A \\ B \end{pmatrix} = \begin{pmatrix} 0 \\ 0 \end{pmatrix}, \tag{6.56}$$

which has a nontrivial solution if and only if

$$\begin{vmatrix} \lambda^2\epsilon^2 + c\epsilon\lambda - 1 & -1 \\ 1 & c\lambda \end{vmatrix} = 0. \tag{6.57}$$

Hence, λ must be a root of the characteristic polynomial

$$\epsilon^2 p(\lambda) = \epsilon^2\lambda^3 + \epsilon c\lambda^2 - \lambda + 1/c = 0. \tag{6.58}$$

There is exactly one negative root, call it λ_1, and the real parts of the other two roots, λ_2 and λ_3, are positive.

In region II, the differential equation is

$$\epsilon^2 v_{\xi\xi} + c\epsilon v_\xi + 1 - v - w = 0, \tag{6.59}$$

$$cw_\xi + v = 0. \tag{6.60}$$

The inhomogeneous solution is $w = 1, v = 0$, and the homogeneous solution is a sum of exponentials of the form $e^{\lambda_i\xi}$.

Since we want the solution to approach zero in the limit $\xi \to \pm\infty$, the traveling pulse can be represented as the exponential $e^{\lambda_1\xi}$ for large positive ξ, the sum of the two exponentials $e^{\lambda_2\xi}$ and $e^{\lambda_3\xi}$ for large negative ξ, and the sum of all three exponentials for the intermediate range of ξ for which $v(\xi) > \alpha$. We take

$$w(\xi) = \begin{cases} Ae^{\lambda_1\xi}, & \text{for} \quad \xi \geq \xi_1, \\ 1 + \displaystyle\sum_{i=1}^{3} B_i e^{\lambda_i\xi}, & \text{for} \quad 0 \leq \xi \leq \xi_1, \\ \displaystyle\sum_{i=2}^{3} C_i e^{\lambda_i\xi}, & \text{for} \quad \xi \leq 0, \end{cases} \tag{6.61}$$

with $v = -cw_\xi$. We also require $w(\xi), v(\xi)$, and $v_\xi(\xi)$ to be continuous at $\xi = 0, \xi_1$, and that $v(0) = v(\xi_1) = \alpha$.

There are six unknown constants and two unknown parameters c and ξ_1 that must be determined from the six continuity conditions and the two constraints. Following some calculation, we eliminate the coefficients A, B_i, and C_i, leaving the two constraints

$$e^{\lambda_1\xi_1} + \epsilon^2 p'(\lambda_1)\alpha - 1 = 0, \tag{6.62}$$

$$\frac{e^{-\lambda_2\xi_1}}{p'(\lambda_2)} + \frac{e^{-\lambda_3\xi_1}}{p'(\lambda_3)} + \frac{1}{p'(\lambda_1)} + \epsilon^2\alpha = 0. \tag{6.63}$$

There are now two unknowns, c and ξ_1, and two equations. In general, (6.62) could be solved for ξ_1, and (6.63) could then be used to determine c for each fixed α and ϵ.

However, it is more convenient to treat c as known and α as unknown, and then find α as a function of c. So, we set $s = e^{\lambda_1 \xi_1}$, in which case (6.63) becomes

$$h(s) = 2 - s + \frac{p'(\lambda_1)}{p'(\lambda_2)} e^{-\lambda_2 \ln(s)/\lambda_1} + \frac{p'(\lambda_1)}{p'(\lambda_3)} e^{-\lambda_3 \ln(s)/\lambda_1} = 0, \tag{6.64}$$

where α has been eliminated using (6.62). We seek a solution of $h(s) = 0$ with $0 < s < 1$.

We begin by noting that $h(0) = 2, h(1) = 0, h'(1) = 0$, and $h''(1) = p'(\lambda_1)/\lambda_1^2 - 2$. The first of these relationships follows from the fact that the real parts of λ_2 and λ_3 are of different sign from λ_1, and therefore, in the limit as $s \to 0$, the exponential terms disappear as the real parts of the exponents approach $-\infty$. The second relationship, $h(1) = 0$, follows from the fact that $1/p'(\lambda_1) + 1/p'(\lambda_2) + 1/p'(\lambda_3) = 0$ (Exercise 9). The final two relationships are similar and are left as exercises (Exercises 9, 10).

If $h''(1) < 0$, then the value $s = 1$ is a local maximum of $h(s)$, so for s slightly less than 1, $h(s) < 0$. Since $h(0) > 0$, a root of $h(s) = 0$ in the interval $0 < s < 1$ is assured.

When λ_2 and λ_3 are real, $h(s)$ can have at most one inflection point in the interval $0 < s < 1$. This follows because the equation $h''(s) = 0$ can be written in the form $e^{(\lambda_2 - \lambda_3)\xi_1} = c$, which can have at most one root. Thus, if $h''(1) < 0$ there is precisely one root, while if $h''(1) > 0$ there can be no roots. If the roots λ_2 and λ_3 are complex, uniqueness is not assured, although the condition $h''(1) < 0$ guarantees that there is at least one root.

Differentiating the defining polynomial (6.58) with respect to λ, we observe that the condition $h''(1) < 0$ is equivalent to requiring $\epsilon^2 \lambda_1^2 + 2c\epsilon\lambda_1 - 1 < 0$. Furthermore, from the defining characteristic polynomial, we know that $\epsilon^2 \lambda_1^2 - 1 = -c\epsilon\lambda_1 + \epsilon^2/(\lambda_1 c)$, and thus it follows that $h''(1) < 0$ if $\lambda_1 < -\frac{1}{c\sqrt{\epsilon}}$. Since the polynomial $p(\lambda)$ is increasing at λ_1, we are assured that $\lambda_1 < -\frac{1}{c\sqrt{\epsilon}}$ if $p(-\frac{1}{c\sqrt{\epsilon}}) > 0$, i.e., if

$$c^2 > \epsilon. \tag{6.65}$$

Thus, whenever $c > \sqrt{\epsilon}$, a root of $h(s) = 0$ with $0 < s < 1$ is guaranteed to exist.

Once s is known, α can be found from the relationship (6.62) whereby

$$\alpha = \frac{1 - s}{\epsilon^2 p'(\lambda_1)}. \tag{6.66}$$

In Fig. 6.5, we show the results of solving (6.64) numerically. Shown plotted is the speed c against α for three values of ϵ. The dashed curve is the asymptotic limit (6.12) for the curves in the limit $\epsilon \to 0$. The important feature to notice is that for each value of α and ϵ small enough there are two traveling pulses, while for large α there are no traveling pulses. In Fig. 6.6A is shown the fast traveling pulse, and in Fig. 6.6B is shown the slow traveling pulse, both for $\alpha = 0.1, \epsilon = 0.1$, and with $v(\xi)$ shown solid and $w(\xi)$ shown dashed.

Note that the amplitude of the slow pulse in Fig. 6.6B is substantially smaller than that of the fast pulse in Fig. 6.6A. Generally speaking, the fast pulse is stable (Jones, 1984; Yanagida, 1985), and the slow pulse is unstable (Maginu, 1985). Also note that there is nothing in the construction of these wave solutions requiring ϵ to be small.

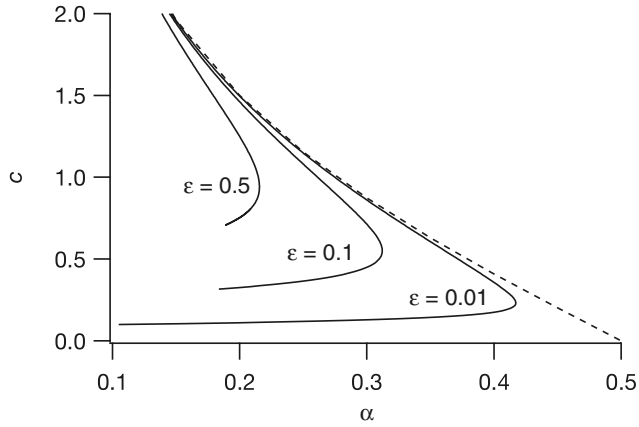

Figure 6.5 Speed c as a function of α for the traveling pulse solution of the piecewise-linear FitzHugh–Nagumo system, shown for $\epsilon = 0.5, 0.1, 0.01$. The dashed curve shows the asymptotic limit as $\epsilon \to 0$, found by singular perturbation arguments.

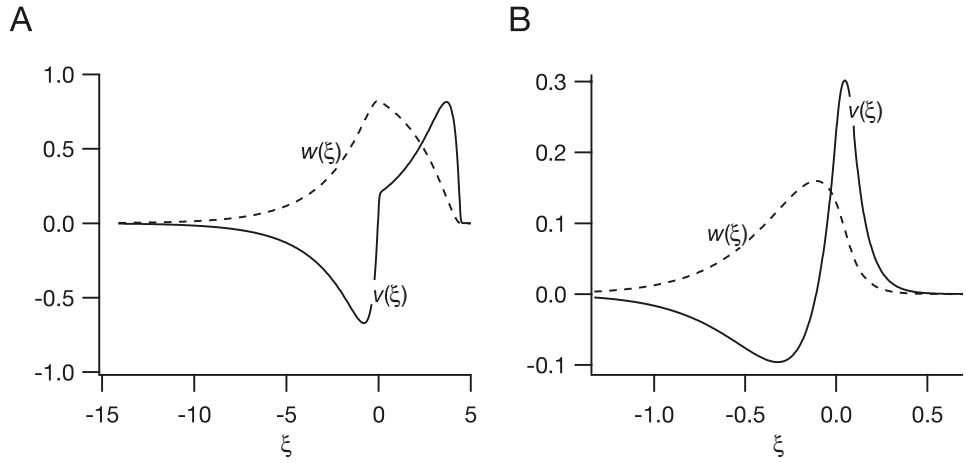

Figure 6.6 A: Plots of $v(\xi)$ and $w(\xi)$ for the fast traveling pulse ($c = 2.66$) for the piecewise-linear FitzHugh–Nagumo system with $\alpha = 0.1, \epsilon = 0.1$. B: Plots of $v(\xi)$ and $w(\xi)$ for the slow traveling pulse ($c = 0.34$) for the same piecewise-linear FitzHugh–Nagumo system as in panel A.

Singular Perturbation Theory

The next way to extract information about the traveling pulse solution of (6.48)–(6.49) is to exploit the smallness of the parameter ϵ (Keener, 1980a; for a different approach, see Rauch and Smoller, 1978). One reason we expect this to be fruitful is because of similarities with the phase portrait of the FitzHugh–Nagumo equations without

diffusion, shown in Fig. 5.15. By analogy, we expect the solution to stay close to the nullcline $f(v,w) = 0$ wherever possible, with rapid transitions between the two outer branches.

The details of this behavior follow from singular perturbation analysis. (This analysis was first given for a simplified FitzHugh–Nagumo system by Casten et al., 1975.) The first observation follows simply from setting ϵ to zero in (6.48). Doing so, we obtain the *outer equations*

$$w_t = g(v,w), \qquad f(v,w) = 0. \tag{6.67}$$

Because the equation $f(v,w) = 0$ is assumed to have three solutions for v as a function of w, and only two of these solutions, the upper and lower solution branches, are stable (cf. Fig. 5.13 and the discussion in Section 5.2), the outer equations (6.67) reduce to

$$\frac{\partial w}{\partial t} = G_{\pm}(w). \tag{6.68}$$

A region of space in which $v = V_+(w)$ is called an *excited region*, and a region in which $v = V_-(w)$ is called a *recovering region*. The outer equation is valid whenever diffusion is not large. However, we anticipate that there are regions of space (*interfaces*) where diffusion is large and in which (6.68) cannot be correct.

To find out what happens when diffusion is large we rescale space and time. Letting $y(t)$ denote the position of the wave front, we set $\tau = t$ and $\xi = \frac{x-y(t)}{\epsilon}$, after which the original system of equations (6.48)–(6.49) becomes

$$v_{\xi\xi} + y'(\tau)v_\xi + f(v,w) = \epsilon\frac{\partial v}{\partial \tau}, \tag{6.69}$$

$$-y'(\tau)w_\xi = \epsilon\left(g(v,w) - \frac{\partial w}{\partial \tau}\right). \tag{6.70}$$

Upon setting $\epsilon = 0$, we find the reduced *inner equations*

$$v_{\xi\xi} + y'(\tau)v_\xi + f(v,w) = 0, \tag{6.71}$$

$$y'(\tau)w_\xi = 0. \tag{6.72}$$

Even though the inner equations (6.71)–(6.72) are partial differential equations, the variable τ occurs only as a parameter, and so (6.71)–(6.72) can be solved as if they were ordinary differential equations. This is because the traveling wave is stationary in the moving coordinate system ξ, τ. It follows that w is independent of ξ (but not necessarily τ). Finally, since the inner equation is supposed to provide a transition layer between regions where outer dynamics hold, we require the *matching condition* that $f(v,w) \to 0$ as $\xi \to \pm\infty$. Note that here we use $y(t)$ to locate the wave front, rather than ct as before, and then $y'(\tau)$ is the instantaneous wave velocity.

We recognize (6.71) as a bistable equation for which there are heteroclinic orbits. That is, for fixed w, if the equation $f(v,w) = 0$ has three roots, two of which are stable as solutions of the equation $dv/dt = f(v,w)$, then there is a number $c = c(w)$ for which

the equation

$$v'' + c(w)v' + f(v,w) = 0 \tag{6.73}$$

has a heteroclinic orbit connecting the two stable roots of $f(v,w) = 0$. This heteroclinic orbit corresponds to a moving transition layer, traveling with speed c. It is important to note that since the roots of $f(v,w) = 0$ are functions of w, c is also a function of w. To be specific, we define $c(w)$ to be the unique parameter value for which (6.73) has a solution with $v \to V_-(w)$ as $\xi \to \infty$, and $v \to V_+(w)$ as $\xi \to -\infty$. In the case that $c(w) > 0$, we describe this transition as an "upjump" moving to the right. If $c(w) < 0$, then the transition is a "downjump" moving to the left.

We are now able to describe a general picture of wave propagation. In most of space, outer dynamics (6.68) are satisfied. At any transition between the two types of outer dynamics, continuity of w is maintained by a sharp transition in v that travels at the speed $y'(t) = c(w)$ if $v = V_-(w)$ on the right and $v = V_+(w)$ on the left, or at speed $y'(t) = -c(w)$ if $v = V_+(w)$ on the right and $v = V_-(w)$ on the left, where w is the value of the recovery variable in the interior of the transition layer. As a transition layer passes any particular point in space, there is a switch of outer dynamics from one to the other of the possible outer solution branches.

This singular perturbation description of wave propagation allows us to examine in more detail the specific case of a traveling pulse. The phase portrait for a solitary pulse is sketched in Fig. 6.7. A traveling pulse consists of a single excitation front followed by a single recovery back. We suppose that far to the right, the medium is at rest, and that a wave front of excitation has been initiated and is moving from left to right. Of course, for the medium to be at rest there must be a rest point of the dynamics on the lower branch, say $G_-(w_+) = 0$. Then, a wave that is moving from left to right has $v = V_-(w_+)$ on its right and $v = V_+(w_+)$ on its left, traveling at speed $y'(t) = c(w_+)$. Necessarily, it must be that $c(w_+) > 0$. Following the same procedure used to derive (6.8), one can show that

$$c(w) = \frac{\int_{V_-(w)}^{V_+(w)} f(v,w)\,dv}{\int_{-\infty}^{\infty} v_\xi^2\,d\xi}, \tag{6.74}$$

and thus $c(w_+) > 0$ if and only if

$$\int_{V_-(w_+)}^{V_+(w_+)} f(v,w_+)\,dv > 0. \tag{6.75}$$

If (6.75) fails to hold, then the medium is not sufficiently excitable to sustain a propagating pulse. It is important also to note that if $f(v,w)$ is of generalized FitzHugh–Nagumo form, then $c(w)$ has a unique zero in the interval (W_*, W^*), where W_* and W^* are defined in Section 5.2.

Immediately to the left of the excitation front, the medium is excited and satisfies the outer dynamics on the upper branch $v = V_+(w)$. Because (by assumption) $G_+(w) > 0$, this can hold for at most a finite amount of time before the outer dynamics force another transition layer to appear. This second transition layer provides a transition

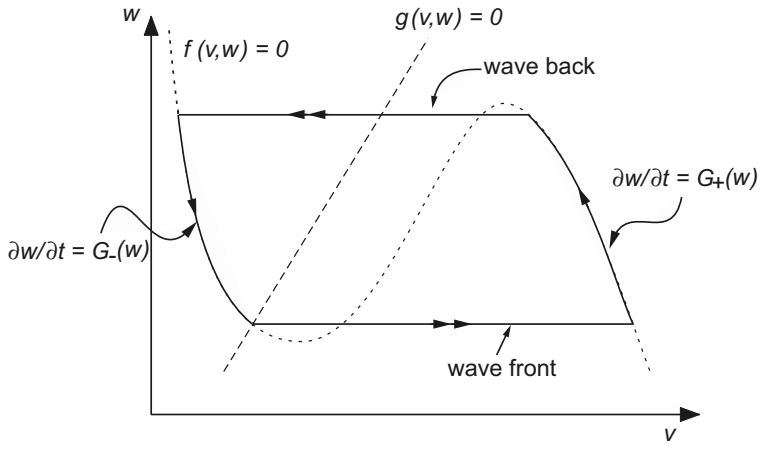

Figure 6.7 Sketch of the phase portrait of the fast traveling solitary pulse for FitzHugh–Nagumo dynamics in the singular limit $\epsilon \to 0$.

between the excited region on the right and a recovering region on the left and travels with speed $y'(t) = -c(w)$, where w is the value of the recovery variable in the transition layer. The minus sign here is because the second transition layer must be a downjump. For this to be a steadily propagating traveling pulse, the speeds of the upjump and downjump must be identical. Thus, the value of w at the downjump, say w_-, must be such that $c(w_-) = -c(w_+)$.

It may be that the equation $c(w_-) = -c(w_+)$ has no solution. In this case, the downjump must occur at the knee, and then the wave is called a *phase wave* since the timing of the downjump is determined solely by the timing, or phase, of the outer dynamics, and not by any diffusive processes. That such a wave can travel at any speed greater than some minimal speed can be shown using standard arguments. The dynamics for phase waves are different from those for the bistable equation because the downjump must be a heteroclinic connection between a saddle point and a saddle-node. That is, at the knee, two of the three steady solutions of the bistable equation are merged into one. The demonstration of the existence of traveling waves in this situation is similar to the case of Fisher's equation, where the nonlinearity $f(v, w)$ in (6.73) has two simple zeros, rather than three as in the bistable case. In the phase wave problem, however, one of the zeros of $f(v, w)$ is not simple, but quadratic in nature, a canonical example of which is $f(v, w) = v^2(1 - v)$. We do not pursue this further except to say that such waves exist (see Exercise 16).

In summary, from singular perturbation theory we learn that the value of w ahead of the traveling pulse is given by the steady-state value w_+, and the speed of the rising wave front is then determined from the bistable equation (6.73) with $w = w_+$. The wave front switches the value of v from $v = V_-(w_+)$ (ahead of the wave) to $v = V_+(w_+)$ (behind the wave front). A wave back then occurs at $w = w_-$, where w_- is determined

from $c(w_-) = -c(w_+)$. The wave back switches the value of v from $v = V_+(w_-)$ to $v = V_-(w_-)$. The duration of the excited phase of the traveling pulse is

$$T_e = \int_{w_+}^{w_-} \frac{dw}{G^+(w)}. \tag{6.76}$$

The duration of the absolute refractory period is

$$T_{\text{ar}} = \int_{w_-}^{w_0} \frac{dw}{G_-(w)}, \tag{6.77}$$

where w_0 is that value of w for which $c(w) = 0$ (Exercise 11). This approximate solution is said to be a singular solution, because derivatives of the solution become infinite (are singular) in the limit $\epsilon \to 0$.

6.3.2 The Hodgkin–Huxley Equations

The traveling pulse for the Hodgkin–Huxley equations must be computed numerically. The most direct way to do this is to simulate the partial differential equation on a long one-dimensional spatial domain. Alternately, one can use the technique of shooting. In fact, shooting was used by Hodgkin and Huxley in their 1952 paper to demonstrate that the Hodgkin–Huxley equations support a traveling wave solution. Shooting is also the method by which a rigorous proof of the existence of traveling waves has been given (Hastings, 1975; Carpenter, 1977).

The shooting argument is as follows. We write the Hodgkin–Huxley equations in the form

$$\tau_m \frac{\partial v}{\partial t} = \lambda_m^2 \frac{\partial^2 v}{\partial x^2} + f(v, m, n, h), \tag{6.78}$$

$$\frac{dw}{dt} = \alpha_w(v)(1 - w) - \beta_w(v)w, \text{ for } w = n, m, \text{ and } h. \tag{6.79}$$

Now we look for solutions in x, t that are functions of the translating variable $\xi = x/c + t$, and find the system of ordinary differential equations

$$\frac{\lambda_m^2}{c^2} \frac{d^2 v}{d\xi^2} + f(v, m, n, h) - \tau_m \frac{dv}{d\xi} = 0, \tag{6.80}$$

$$\frac{dw}{d\xi} = \alpha_w(v)(1 - w) - \beta_w(v)w, \text{ for } w = n, m, \text{ and } h. \tag{6.81}$$

Linearizing the system (6.80) and (6.81) about the resting solution at $v = 0$, one finds that there are four negative eigenvalues and one positive eigenvalue. A reasonable approximation to the unstable manifold is found by neglecting variations in g_{K} and g_{Na}, from which

$$v(t) = v_0 e^{\mu t}, \tag{6.82}$$

where

$$\frac{\lambda_m^2}{c^2}\mu^2 - \tau_m \mu - 1 = 0$$

or

$$\mu = \frac{1}{2}\left(\tau_m \frac{c^2}{\lambda_m^2} + \frac{c}{\lambda_m}\sqrt{\tau_m^2 \frac{c^2}{\lambda_m^2} + 4}\right).$$

To implement shooting, one chooses a value of c, and initial data close to the rest point but on the unstable manifold (6.82), and then integrates numerically until (in all likelihood) the potential becomes very large. It could be that the potential becomes large positive or large negative. In fact, once values of c are found that do both, one uses bisection to home in on the homoclinic orbit that returns to the rest point in the limit $\xi \to \infty$.

For the Hodgkin–Huxley equations one finds a traveling pulse for $c = 3.24\,\lambda_m\ \mathrm{ms}^{-1}$. Using typical values for squid axon (from Table 4.1, $\lambda_m = 0.65$ cm), we find $c = 21$ mm/ms, which is close to the value of 21.2 mm/ms found experimentally by Hodgkin and Huxley. Hodgkin and Huxley estimated the space constant for squid axon as $\lambda_m = 0.58$ cm, from which they calculated that $c = 18.8$ mm/ms. Their calculated speeds agreed very well with experimental data and thus their model, which was based only on measurements of ionic conductance, was used to predict accurately macroscopic behavior of the axon. It is rare that quantitative models can be applied so successfully. Propagation velocities for several types of excitable tissue are listed in Table 6.2.

Table 6.2 Propagation velocities in nerve and muscle.

Excitable Tissue	Velocity (m/sec)
Myelinated nerve fibers	
Large diameter (16–20 μm)	100–120
Mid-diameter (10–12 μm)	60–70
Small diameter (4–6 μm)	30–50
Nonmyelinated nerve fibers	
Mid-diameter (3–5 μm)	15–20
Skeletal muscle fibers	6
Heart	
Purkinje fibers	1.0
Cardiac muscle	0.5
Smooth muscle	0.05

6.4 Periodic Wave Trains

Excitable systems are characterized by both excitability and refractoriness. That is, after the system has responded to a superthreshold stimulus with a large excursion from rest, there is a refractory period during which no subsequent responses can be evoked, followed by a recovery period during which excitability is gradually restored. Once excitability is restored, another wave of excitation can be evoked. However, the speed at which subsequent waves of excitation travel depends strongly on the time allowed for recovery of excitability following the last excitation wave. Generally (but not always), the longer the period of recovery, the faster the new wave of excitation can travel.

One might guess that a nerve axon supports, in addition to a traveling pulse, periodic wave trains of action potentials. With a periodic wave train, if recovery is a monotonic process, one expects propagation to be slower than for a traveling pulse, because subsequent action potentials occur before the medium is fully recovered, so that the Na^+ upstroke is slower than for a traveling pulse. The relationship between the speed and period is called the *dispersion curve*.

There are at least two ways to numerically calculate the dispersion curve for the Hodgkin–Huxley equations. The most direct method is to construct a ring, that is, a one-dimensional domain with periodic boundary conditions, initiate a pulse that travels in one direction on the ring, and solve the equations numerically until the solution becomes periodic in time. One can then use this waveform as initial data for a ring of slightly different length, and do the calculation again. While this method is relatively easy, its principal disadvantage is that it requires the periodic solution to be stable. Dispersion curves often have regions whose periodic solutions are unstable, and this method cannot find those. Of course, only the stable solutions are physically realizable, so this disadvantage may not be so serious to the realist.

The second method is to look for periodic solutions of the equations in their traveling wave coordinates (6.80)–(6.81), using a numerical continuation method (an automatic continuation program such as AUTO recommends itself here). With this method, periodic solutions are found without reference to their stability, so that the entire dispersion curve can be calculated.

Dispersion curves for excitable systems have a typical shape, depicted in Figs. 6.8 and 6.9. Here we see a dispersion curve having two branches, one denoting fast waves, the other slow. The two branches meet at a knee or corner at the *absolute refractory period*, and for shorter periods no periodic solutions exist. The solutions on the fast branch are typical of action potentials and are usually (but not always) stable. The solutions on the slow branch are small amplitude oscillations and are unstable.

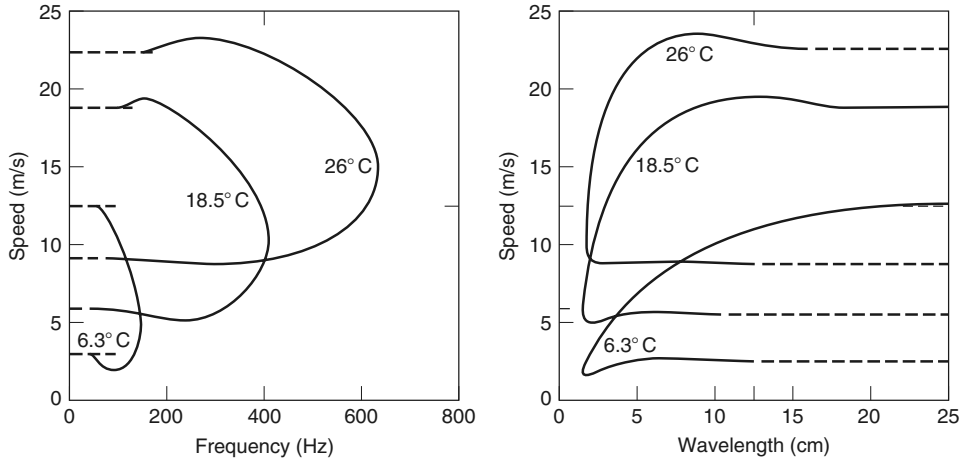

Figure 6.8 Numerically computed dispersion curve (speed vs. frequency and speed vs. wavelength for various temperatures) for the Hodgkin–Huxley equations. (Miller and Rinzel, 1981, Figs. 1 and 2.)

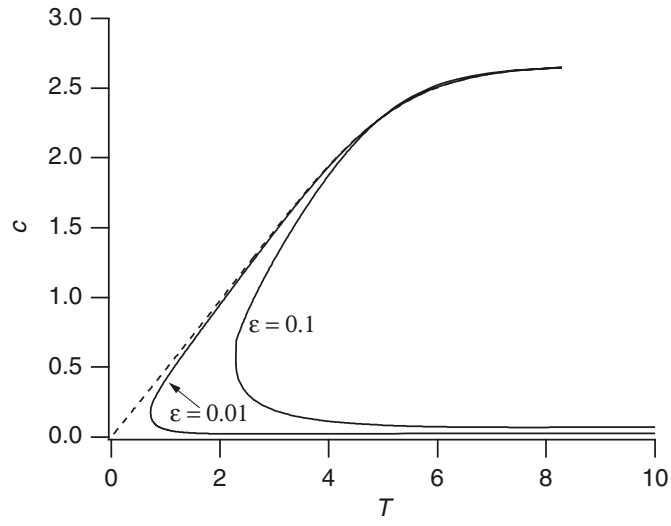

Figure 6.9 Dispersion curves for the piecewise-linear FitzHugh–Nagumo equations shown for $\epsilon = 0.1$ and 0.01. The dashed curve shows the singular perturbation approximation to the dispersion curve.

6.4.1 Piecewise-Linear FitzHugh–Nagumo Equations

The dispersion curve in Fig. 6.9 was found for the FitzHugh–Nagumo system (6.48)–(6.49) with piecewise-linear functions (6.52) and (6.53). The calculation is similar to

that for the traveling pulse (Rinzel and Keller, 1973). Since this system is piecewise linear, we can express its solution as the sum of three exponentials,

$$w(\xi) = \sum_{i=1}^{3} A_i e^{\lambda_i \xi}, \tag{6.83}$$

on the interval $0 \le \xi < \xi_1$, and as

$$w(\xi) = 1 + \sum_{i=1}^{3} B_i e^{\lambda_i \xi} \tag{6.84}$$

on the interval $\xi_1 \le \xi \le \xi_2$, where $v = -cw_\xi$. We also assume that $v > \alpha$ on the interval $\xi_1 \le \xi \le \xi_2$. The numbers $\lambda_i, i = 1, 2, 3$, are roots of the characteristic polynomial (6.58).

We require that $w(\xi), v(\xi)$, and $v'(\xi)$ be continuous at $\xi = \xi_1$, and that $w(0) = w(\xi_2), v(0) = v(\xi_2)$, and $v'(0) = v'(\xi_2)$ for periodicity. Finally, we require that $v(0) = v(\xi_1) = \alpha$. This gives a total of eight equations in nine unknowns, $A_1, \ldots, A_3, B_1, \ldots, B_3$, ξ_1, ξ_2, and c. After some calculation we find two equations for the three unknowns ξ_1, ξ_2, and c given by

$$\frac{e^{\lambda_1(P-\xi_1)} - 1}{p'(\lambda_1)(e^{\lambda_1 P} - 1)} + \frac{e^{\lambda_2(P-\xi_1)} - 1}{p'(\lambda_2)(e^{\lambda_2 P} - 1)} + \frac{e^{\lambda_3(P-\xi_1)} - 1}{p'(\lambda_3)(e^{\lambda_3 P} - 1)} + \epsilon^2\alpha = 0, \tag{6.85}$$

$$\frac{e^{\lambda_1 P} - e^{\lambda_1 \xi_1}}{p'(\lambda_1)(e^{\lambda_1 P} - 1)} + \frac{e^{\lambda_2 P} - e^{\lambda_2 \xi_1}}{p'(\lambda_2)(e^{\lambda_2 P} - 1)} + \frac{e^{\lambda_3 P} - e^{\lambda_3 \xi_1}}{p'(\lambda_3)(e^{\lambda_3 P} - 1)} + \epsilon^2\alpha = 0, \tag{6.86}$$

where $P = \xi_2/c$. It is important to note that since there are only two equations for the three unknowns, (6.85) and (6.86) define a family of periodic waves, parameterized by either the period or the wave speed. The relationship between the period and the speed of this wave family is the dispersion curve. In Fig. 6.9 are shown examples of the dispersion curve for a sampling of values of ϵ with $\alpha = 0.1$. Changing α has little qualitative effect on this plot. The dashed curve shows the limiting behavior of the upper branch (the fast waves) in the limit $\epsilon \to 0$. Of significance in this plot is the fact that there are fast and slow waves, and in the limit of large wavelength, the periodic waves approach the solitary traveling pulses represented by Fig. 6.5 (Exercise 12). In fact, periodic solutions look much like evenly spaced periodic repeats of (truncated) solitary pulses.

The dispersion curve for the piecewise-linear FitzHugh–Nagumo system is typical of dispersion curves for excitable media, with a fast and slow branch meeting at a corner. In general, the location of the corner depends on the excitability of the medium (in this case, the parameter α) and on the ratio of time scales ϵ.

6.4.2 Singular Perturbation Theory

The fast branch of the dispersion curve can be found for a general FitzHugh–Nagumo system in the limit $\epsilon \to 0$ using singular perturbation theory. A periodic wave consists of an alternating series of upjumps and downjumps, separated by regions of outer

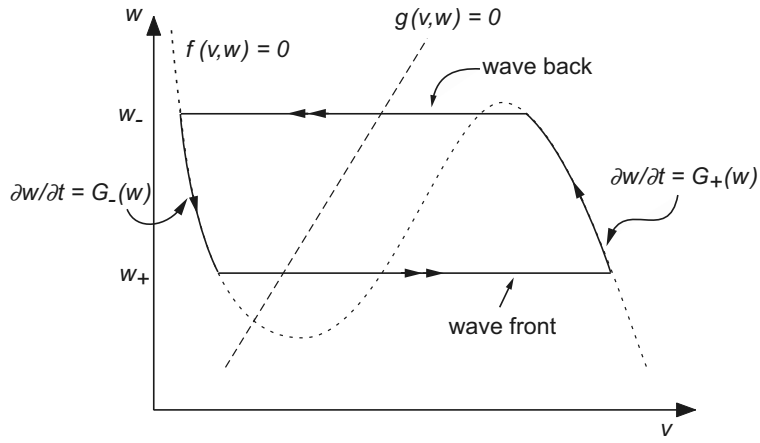

Figure 6.10 Sketch of the phase portrait for the fast traveling periodic wave train for FitzHugh–Nagumo dynamics in the singular limit $\epsilon \to 0$.

dynamics. The phase portrait for a periodic wave train is sketched in Fig. 6.10. To be periodic, if w_+ is the value of the recovery variable in the upjump, traveling with speed $c(w_+)$, then the value of w in the downjump must be w_-, where $c(w_+) = -c(w_-)$. The amount of time spent on the excited branch is

$$T_e = \int_{w_+}^{w_-} \frac{dw}{G_+(w)}, \tag{6.87}$$

and the amount of time spent on the recovery branch is

$$T_r = \int_{w_-}^{w_+} \frac{dw}{G_-(w)}. \tag{6.88}$$

The dispersion curve is then the relationship between speed $c(w_+)$ and period

$$T = T_e + T_r, \tag{6.89}$$

parameterized by w_+. This approximate dispersion curve (calculated numerically) is shown in Fig. 6.9 as a dashed curve.

The slow branch of the dispersion curve can also be found using perturbation methods, although in this case since the speed is small of order ϵ, a regular perturbation expansion is appropriate. The details of this expansion are beyond the scope of this book, although the interested reader is referred to Dockery and Keener (1989). In general, the slow periodic solutions are unstable (Maginu, 1985) and therefore are of less physical interest than the fast solutions. Again, stability theory for the traveling wave solutions is beyond the scope of this book.

6.4.3 Kinematics

Not all waves are periodic. There can be wave trains with action potentials that are irregularly spaced and that travel with different velocities. A *kinematic theory* of wave propagation is one that attempts to follow the progress of individual action potentials without tracking the details of the structure of the pulse (Rinzel and Maginu, 1984). The simplest kinematic theory is to interpret the dispersion curve in a local way. That is, suppose we know the speed as a function of period for the stable periodic wave trains, $c = C(T)$. We suppose that the wave train consists of action potentials, and that the nth action potential reaches position x at time $t_n(x)$. To keep track of time of arrival at position x we note that

$$\frac{dt_n}{dx} = \frac{1}{c}. \tag{6.90}$$

We complete the description by taking $c = C(t_n(x) - t_{n-1}(x))$, realizing that $t_n(x) - t_{n-1}(x)$ is the instantaneous period of the wave train that is felt by the medium at position x.

A more sophisticated kinematic theory can be derived from the singular solution of the FitzHugh–Nagumo equations. For this derivation we assume that recovery is always via a phase wave, occurring with recovery value W^*. Suppose that the front of the nth action potential has speed $c(w_n)$, corresponding to the recovery value w_n in the transition layer. Keeping track of the time until the next action potential, we find

$$t_{n+1}(x) - t_n(x) = T_e(x) + T_r(x) \tag{6.91}$$

$$= \int_{w_n}^{W^*} \frac{dw}{G_+(w)} + \int_{W^*}^{w_{n+1}} \frac{dw}{G_-(w)}. \tag{6.92}$$

Differentiating (6.92) with respect to x, we find the differential equation for $w_{n+1}(x)$:

$$\frac{1}{G_-(w_{n+1})}\frac{dw_{n+1}}{dx} = \frac{1}{G_+(w_n)}\frac{dw_n}{dx} + \frac{1}{c(w_{n+1})} - \frac{1}{c(w_n)}. \tag{6.93}$$

With this equation one can track the variable w_{n+1} as a function of x given $w_n(x)$ and from it reconstruct the speed and time of arrival of the $(n+1)$st action potential wave front.

While this formulation is useful for the FitzHugh–Nagumo equations, it can be given a more general usefulness as follows. Since there is a one-to-one relationship between the speed of a front and the value of the recovery variable w in that front, we can represent these functions in terms of the speeds of the fronts as

$$t_{n+1}(x) - t_n(x) = A(c_n) + t_r(c_{n+1}), \tag{6.94}$$

where $A(c_n) = T_e$ is the *action potential duration* (APD) since the nth upstroke, and $t_r(c_{n+1}) = T_r$ is the recovery time preceding the $(n+1)$st upstroke. When we differentiate this conservation law with respect to x, we find a differential equation for the speed of

the $(n+1)$st wave front as a function of the speed of the nth wave front, given by

$$t_r'(c_{n+1})\frac{dc_{n+1}}{dx} = \frac{1}{c_{n+1}} - \frac{1}{c_n} - A'(c_n)\frac{dc_n}{dx}. \tag{6.95}$$

The advantage of this formulation is that the functions A and t_r may be known for other reasons, perhaps from experimental data. It is generally recognized that the action potential duration is functionally related to the speed of the previous action potential, and it is also reasonable that the speed of a subsequent action potential can be related functionally to the time of recovery since the end of the last action potential. Thus, the model (6.95) has applicability that goes beyond the FitzHugh–Nagumo context. For an example of how this idea has been used for the Beeler–Reuter dynamics, see Courtemanche et al. (1996).

6.5 Wave Propagation in Higher Dimensions

Not all excitable media can be viewed as one-dimensional cables, neither is all propagated activity one-dimensional. Tissues for which one-dimensional descriptions of cellular communication are inadequate include skeletal and cardiac tissue, the retina, and the cortex of the brain. To understand communication and signaling in these tissues requires more complicated mathematical analysis than for one-dimensional cables.

When beginning a study of two- or three-dimensional wave propagation, it is tempting to extend the cable equation to higher dimensions by replacing first derivatives in space with spatial gradients, and second spatial derivatives with the Laplacian operator. Indeed, all the models discussed here are of this type. However, this replacement is not always appropriate.

Some cells, such as *Xenopus* oocytes (frog eggs), are large enough so that waves of chemical activity can be sustained within a single cell. This is unusual, however, as most waves in normal physiological situations serve the purpose of communication between cells. For chemical waves in single cells, a reasonable first guess is that spatial coupling is by chemical diffusion. In that case, if the local chemical dynamics are described by the differential equation $\frac{\partial u}{\partial t} = kf$, then with spatial coupling the dynamics are represented by

$$\frac{\partial u}{\partial t} = \nabla \cdot (D\nabla u) + kf, \tag{6.96}$$

where D is the (scalar) diffusion coefficient of the chemical species and ∇ is the three-dimensional gradient operator. Here we have included the time constant k (with units time^{-1}), so that f has the same dimensional units as u.

For many cell types, however, intercellular communication is through gap junctions between immediate neighbors, so that diffusion is not spatially uniform. In this case, the first guess (or hope) is that the length constant of the phenomenon to be described is much larger than the typical cell size, and homogenization can be used to find an effective diffusion coefficient, D_e, as described in Chapter 8. Then (6.96) with